iJRASET
International Journal For Research in
Applied Science and Engineering Technology

INTERNATIONAL JOURNAL FOR RESEARCH

IN APPLIED SCIENCE & ENGINEERING TECHNOLOGY

Volume: 9 Issue: VIII Month of publication: August 2021

DOI: https://doi.org/10.22214/ijraset.2021.37676

www.ijraset.com

Call: 08813907089 | E-mail ID: ijraset@gmail.com

International Journal for Research in Applied Science & Engineering Technology (IJRASET)
ISSN: 2321-9653; IC Value: 45.98; SJ Impact Factor: 7.429
Volume 9 Issue VIII Aug 2021- Available at www.ijraset.com

Numerical Analysis of Semi-Tangential Ogive Bullet

Avinash T
School of Aeronautical Sciences, Hindustan Institute of Technology and Sciences (HITS), Chennai, avinash3201@gmail.com

Abstract: The objective of the present study is to design and analyze semi-tangential ogive bullets using simulatation software such as Computer-aided design & Computational Fluid Dynamics (CFD). It is observed that been a quite steady increase in the bullet research design in the past few decades. The nose section of ballistic bullet is the most important part of the design process. Hence design optimizations are achieved by adjusting the bullet's form to improve precision and stability by reducing its drag force. CFD is the study used to verify the findings. Since provides most accurate results. It is observed that present study optimizes the behavior of the at M= 2.5. This present work shows the flow of air around the bullet surface providing pressure & velocity contours at every segment. The Various parametric studies over bullet model are drag co-efficient, ballistic coefficient and turbulence viscosity are plotted .

NOMENCLATURE

a	Speed of sound (ft/s)
BC	Ballistic co efficient
C_d	drag Coefficient
GS	Grain structure
M	Mach number
SG	Stability factor
TR	Twist rate(in)
VLD	Very low drag
U	Velocity component along body (ft/s)
ρ	Ogive radius(in)
r_n	Nose radius(in)
x_a	Meplat length(in)
$\hat{v}$	Turbulence kinematic viscosity Ft^2T^{-1}
Gv	Turbulence production
Yv	Turbulence destruction
$\sigma\hat{v}$	Indicate constants.

I. INTRODUCTION

Many factors influence the consistency and precision of a bullet's motion in order for it to achieve its target location, so an approach to mitigate inaccuracy and to make the bullet's motion stable needs to be designed. Hence some consideration has been given about how the bullet configuration might be improved. According to recent studies by Litz [1], VLD bullets have seen a increase in accuracy for long-range shooters on targets due to the presence of low drag and high ballistic coefficient of bullet model. Tangent ogive bullet allows the bullet to self align due to the smooth junctures along with good bearing surface. But tangent ogive provides which need to reduce.

in order to have lower drag and high BC compared to tangent ogive bullets secant ogive are developed , But the abrupt junctures between the bearing surface prevent the bullet from self aligning during its flight. The benefit of present study over tangent and secant ogive architecture will improves aim accuracy and long-range shooting. The explanation for the advancement of semi-tangential bullets is as follows: is the combined of the tangent ogive from a bullet's bearing surface is unaffected by seating distance, while the continuous secant ogive, which is equal to VLD, provides a high BC and low drag Style projectiles.

This paper adds to the current research series by performing a computational investigation of semi-tangential blend type aim bullets to determine their aerodynamic characteristics and compare results. The expression "ogive" refers to the point at which the curve reaches the bullet diameter. The arc radius of an ogive is commonly used to describe it. The typical or secant ogive is a circular surface of revolution formed by the same curve that forms a Gothic arch. Greater radius than the diameter of the cylindrical section where else in case of tangent ogive. If the ogive is said to be perfectly tangent, then the curve is defined by its own very specific radius

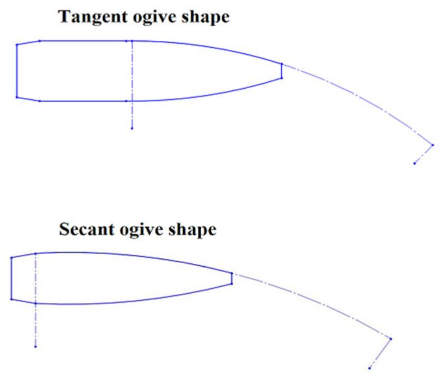

Fig 1: Tangent and secant ogive bullet

II. LITERATURE SURVEY

This literature survey shows a huge research effort to characterize the aerodynamic performance of bullets and their ballistics. From the research work of Litz [1] chateretics of different bullet shapes has been found, the research says about the advantages and disadvantages of various bullet shapes. But the research does not discuss the flow parameters of the bullet shapes. In the research works of Narayan [2].flow past over various nose geometry gives us a detailed view of flow over different nose geometry & gives a clear vision of the shock generated by the nose shapes. in the research thesis of Wilcox [3] Formulation of the k-w Turbulence Model, explains about the k-omega turbulence model uses an approximation for the Reynolds-averaged Navier–Stokes equations in computational fluid dynamics (RANS equations). The model uses two partial differential equations for two variables, k, and ω**,** to try to predict turbulence. The physical parameters of other ogive bullet is taken from Berger bullet catalog [4] .in order to perform a comparative study of different turbulent model, A One Equation Turbulence Model for Aerodynamic Flows [5] by Spalart & Allmaras is used to the study. In the researches of [6] Rebecca, the influence of the bullet shape on the width of abrasion collars, gives a detailed view about the abrasion created by different bullet shapes in human body. From the research article of Petzal [7]. Field and Stream is one of the pioneer research which gives a expanded view on the flow of bullet in air with a visual presentation of shockwaves, wake region, shear layer generated during bullet flow. The velocity contour & turbulence intensity of the hybrid ogive was first discussed in Muruganantham & Babin[8] , but the shockwave generation is not discussed in the journal. But in Menezes, & Maruta[9], Hypersonic flow over a multi-step after body gives us a detailed view about the shock wave generation at hypersonic speed in bullet body, which intern made us identify the shockwave generated in our bullet design. Since the ogive design of us have blunt nose character, the necessary data for flow over a blunt nose shape is taken from the researches Owens[10]. Aerodynamic characteristics of spherically blunted cones at Mach numbers from 0.5 to 5.0 where the location of the bow shock wave is been noted. But the ogive design has both blunt & parabolic shape, hence both bow shockwave & attached shockwave may generation. The location of the shockwave has been found using this research Heberle, & Goodrum, PB[11]. Data on shape and location of detached shock waves on cones and spheres. The ability of bow shock to detach the heat generated into the atmosphere without interfering with the bullet structure is found out by Fay & Riddell[12]. Theory of stagnation point heat transfer in dissociated air Shock Waves. From the researches of Raghuraman & Govardhan[13], study shock wave-boundary layer interaction Instantaneous schlieren images show the formation of a series of compression waves inside the boundary layer and these waves combine to form a separation shock wave outside the boundary layer, with the nature of these shocks varying with time, from the effect of the shock wave to the boundary layer has been noted Seshadri and A. De [14] The flow simulation models, visualization view like contour, vector arrow are been discussed in the researches of Torii [15] & [18] The present study reports on flow past airfoils (stationary and moving) using sharp interface immersed-boundary approach. A non-boundary conforming approach like the immersed-boundary method offers a viable alternative over the traditional boundary conforming approach by allowing us to model flow past arbitrarily complex shapes, by eliminating the need to re-grid the flow domain as the body exhibits motion .the efficiency of drag calculated in CFD is been studied and the results have been found by Suvranu De, Efficient Computation of Fluid Drag Forces on Micro machined Devices Using a Boundary Integral Equation-Based Approach S. De [16].the design techniques and methodology for complex structure are mentioned in the research of Braun & Wright[17]. The problems that are faced during the flow simulation are explained and how does a bullet behaves inflow by rotating its air are been discussed in Donea, J., and Huerta [19]& [20] by which the turning ratio value of the bullet is calculated. From the research of S. K, B. K, P. Selvarajan [21] drag reduction study of a 2D metal projectile series using SU2 code, implementing of boat tail design to the trailing edge of the bullet has a great influence on the turbulence and the drag reduction by reducing the turbulence intensity by converging the flow quickly and which intend to reduce the form drag generated.

III. MODEL SPECIFICATIONS

The model specification are mentioned in the below table. The dimension mentioned in the table is in inches

Table 1: Bullet dimensions

Specification	30 cal/ 0.308 266GR
Bullet Diameter (1)	0.308in
Boat Tail (2)	0.217in
Bearing Surface (3)	0.467in
Base To Ogive (4)	0.684in
Nose Length (5)	0.891in
Meplat (6)	0.070in
Tail Length (7)	0.280in

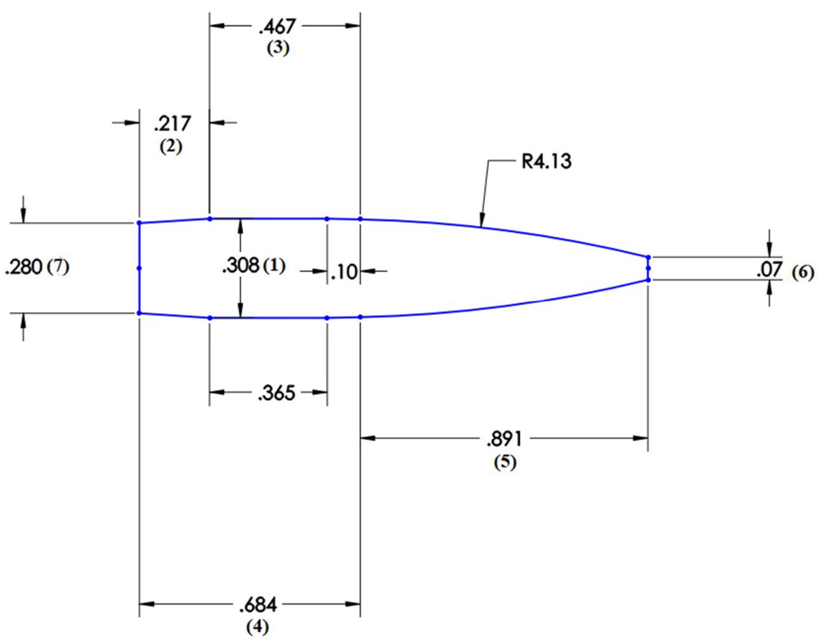

Fig 2: Bullet dimensions [Table 1]

Table 2: Values Of 30 Caliber Semi-Tangentail Bullet

GRAIN STRUCTURE	266gr
BALLISTIC CO-EFFICENT (G7)	0.422
TWIST RATE	1/10"
RPM OF BULLET	201600
STABLITY FACTOR	1.8
OGIVE TYPE	SEMI-TANGENTIAL
OAL(OVERALL LENGTH)	1.575 in
BASE STYLE	Boat Tail

A. Flows Past Over Various Bullet Shapes

The flow past different geometry forms of the nose has been completed, according to the study of Narayan [2]. The Mach number contours of a spherically blunted nose and a parabolic nose have been obtained as a result of the testing. In the contours of a spherically blunted nose The bow shock structure near the nose, which involves strong and fragile regions of the bow shock. A sonic line separates the flow, allowing it to reaccelerate to supersonic level. Instead of involving the flow abruptly slows from hypersonic to subsonic due to a strong and thin natural shock that forms near the blunted flow. They were successful in getting The flow path can be observed after a deceleration in front of the current simulation, as previously stated. The blunted nose is accompanied by re-acceleration from the nose cone's horizontally, as it was before. Shock positions that match ahead of the abrupt change in Mach number are seen as blunted nose cones, and static pressure plots with high gradients are labeled with an ellipse. The attached shock has little impact on the abrupt jump. In the parabolic nose cone; instead, small leaps with poor gradients can be seen in the Mach number and static pressure plots. Since a parabolic nose has a lower aerodynamic drag than a spherically blunted one.

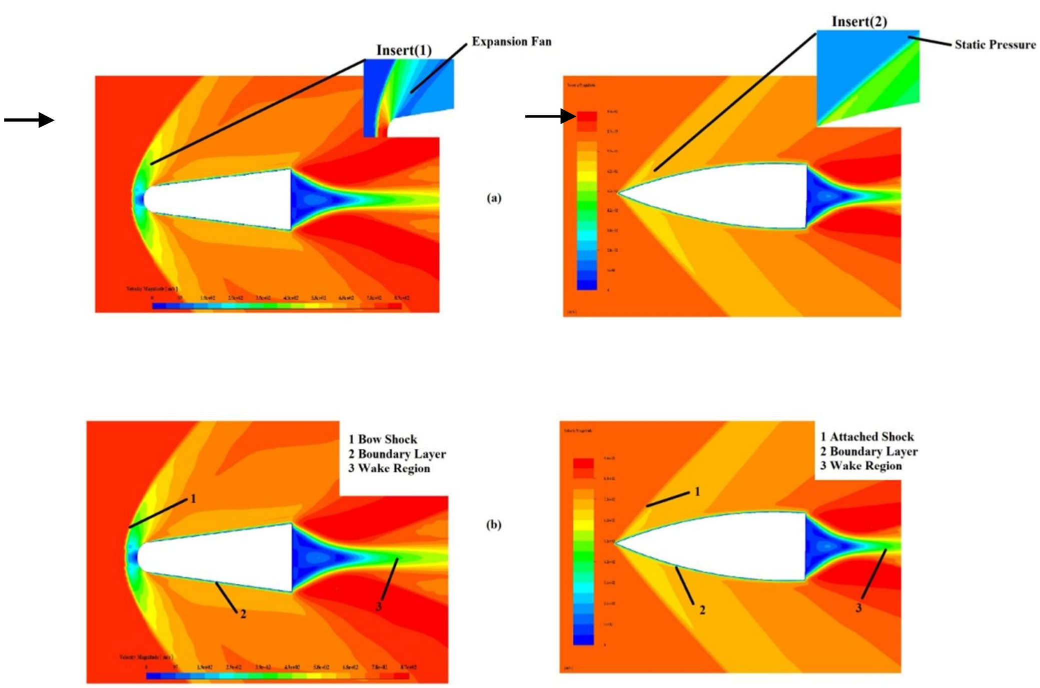

Fig 3: flow past over various bullet shapes

International Journal for Research in Applied Science & Engineering Technology (IJRASET)
ISSN: 2321-9653; IC Value: 45.98; SJ Impact Factor: 7.429
Volume 9 Issue VIII Aug 2021- Available at www.ijraset.com

IV. MESHING & MODEL

Computational fluid dynamics (CFD) is an engineering tool used to simulate the action of thermo-fluids in a system. It is used by many industries in their development work to analyze, optimize and verify the performance of designs before going to prototypes and physical tests.

O-Shape mesh is generated over test subject, with convergence criteria 1e^-05. To achieve good results, O-shaped & structured mesh. A parabolic boundary to the bullet is created using an appropriate CAD platform. The length of this geometry is about 11m. The geometry is a planar surface. It is then split into smaller faces with lines, as can be seen, to create mapped/structured mesh in between them. This geometry is then imported into the solver "Mechanical" meshing plug-in is used. The face meshes (with mapped meshing enabled) are added on each side. The mesh is then generated and viewed. Slight improvements are then made to the sizing inputs to get a good mesh for the solution. Named selections are added and the geometry is then ready to import into the solver.

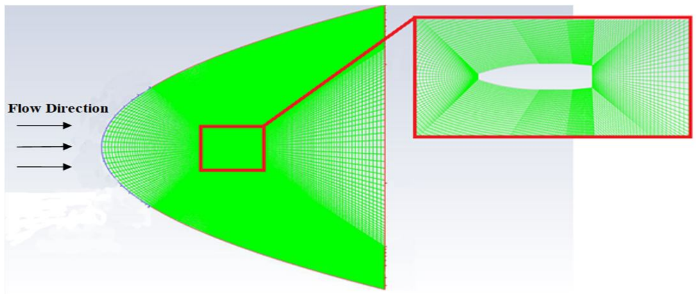

Fig 4: MESHING DOMAIN

A. *Governing Equatation*

The governing equations are PDEs that contain fluid variables which are used to solve fluid flows. According to Wilcox [3], the k–omega turbulence model is a popular two-equation turbulence model that uses an approximation for the Reynolds-averaged Navier–Stokes equations in computational fluid dynamics (RANS equations). The model uses two partial differential equations for two variables, k, and ω, to try to predict turbulence. The first variable is the turbulence kinetic energy (k), while the second (ω) is the specific rate of dissipation (of the turbulence kinetic energy k into internal thermal energy).

$$\frac{\partial(\rho k)}{\partial t}+\frac{\partial(\rho u_j k)}{\partial x_j}=\rho P-\beta^*\rho\omega k+\frac{\partial}{\partial x_j}\left[\left(\mu+\sigma_k\frac{\rho k}{\omega}\right)\frac{\partial k}{\partial x_j}\right] \text{ With } P=\tau_{ij}\frac{\partial u_i}{\partial x_j}$$

$$\frac{\partial(\rho\omega)}{\partial t}+\frac{\partial(\rho u_j\omega)}{\partial x_j}=\frac{\alpha\omega}{k}P-\beta\rho\omega^2+\frac{\partial}{\partial x_j}\left[\left(\mu+\sigma_k\frac{\rho k}{\omega}\right)\frac{\partial k}{\partial x_j}\right]\frac{\partial\omega}{\partial x_j}+\frac{\rho\sigma_d}{\omega}\frac{\partial k}{\partial x_j}$$

B. *Boundary Condition & Mesh Independent Study*

For compressible fluid flow analysis, the reference pressure is set to 0, and the far-field state is subjected to the corresponding gauge pressure (equal to overall pressure). For the flow domain, an ideal gas is selected as the material. TABLE 3, Shows the boundary condition.

Table 3: Boundary Condition

	VALUE/ METHOD
MACH NUMBER	M= 0.50 M= 1 M= 2.5
GAUGE PRESSURE	101325 pa
SOLVER	Steady, Density based
TURBULENCE MODEL	k–omega turbulence model
VISCOSITY MODEL	Sutherland
TEMPERATURE	300K
CONVEGENCE CRITERIA	1e^-5

To achieve an accurate result, a mesh independent study is done for the conditions mentioned in boundary condition .it has been found out that after 150000 element size the value of Cd doesn't change even though the element size is increased

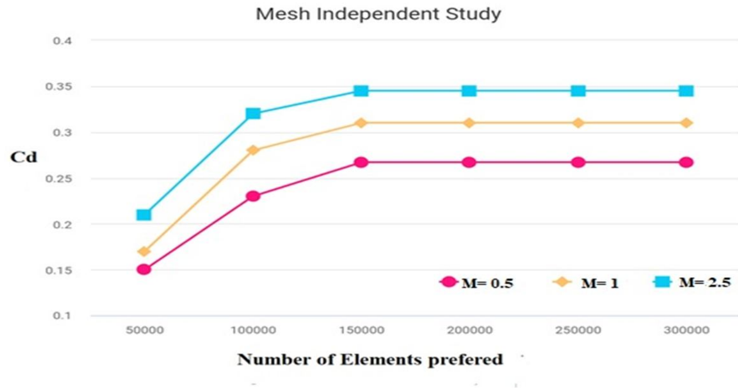

Fig 5: MESH Independent Study

V. RESULTS

The results were obtained using a convergence of 1e^-05 and a total of approx 5K iterations. CFD allows you to simulate the flow distribution over the test subject and compare the effects by plotting the technical parameters along the coordinates. Three separate situations were studied using CFD in three different Mach areas. Drag force was calculated and velocity contour plots were taken to observe the flow distribution around the bullet for aerodynamic efficiency comparison.

The velocity contour graph of a test subject in Mach 0.50 FIG 6, graph shows the formation of wave zone in leading-edge & convergence in trailing edge of a test subject. The velocity contour graph of a test subject in Mach 1.0 FIG 7, the graph shows the formation of wave zone in leading-edge & convergence in trailing edge of a test subject. This also shows the formulation of shockwave in the top and bottom of the test subject a powerful normal shock wave builds up that generates much more heat outside the boundary layer than is the normal case, this shows the test subject is moving from transonic to supersonic. Velocity contour of a test subject at 2.5 Mach. The formulation of the shockwave is at the direction of bullet flow is shown in Figure 8. There is a clear formulation of the bow shock and attached shockwave in Fig 8.

The heat is generated outside the boundary layer surface by shockwave compression. This part is dissipated harmlessly into the surrounding air. The rest of the heat arises within the boundary layer, which is in contact with the bullet structure and has the opportunity to melt or damage the bullet. Structural heating can be reduced if more of the heat can be shifted outside the boundary layer. Since the attached shockwave is away from the boundary layer, where else in the case of the parabolic nose, the attached shockwave is close to the boundary layer in Fig 4, which intern increases the heat of the structure. Where else in semi- tangential bullet shape the generated attached shock does not interfere with boundary layer which reduce the structural heating.

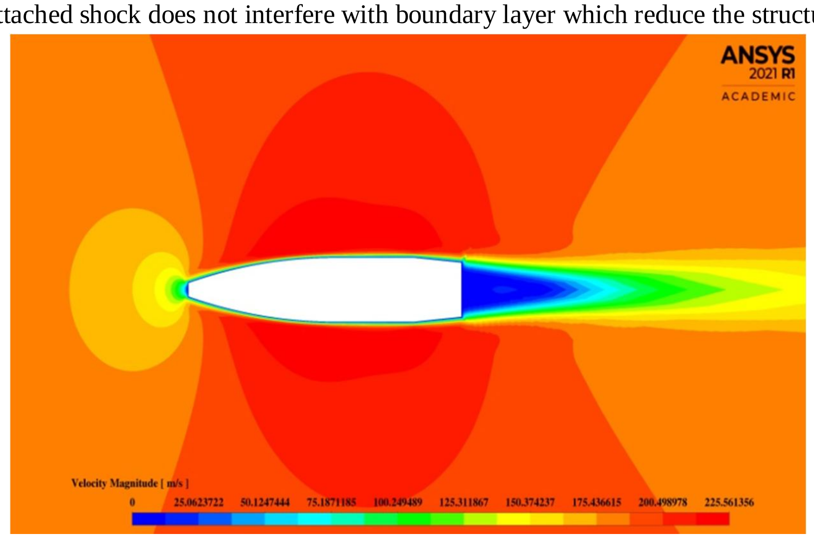

Fig 6: VELOCITY CONTOUR AT M=0.50

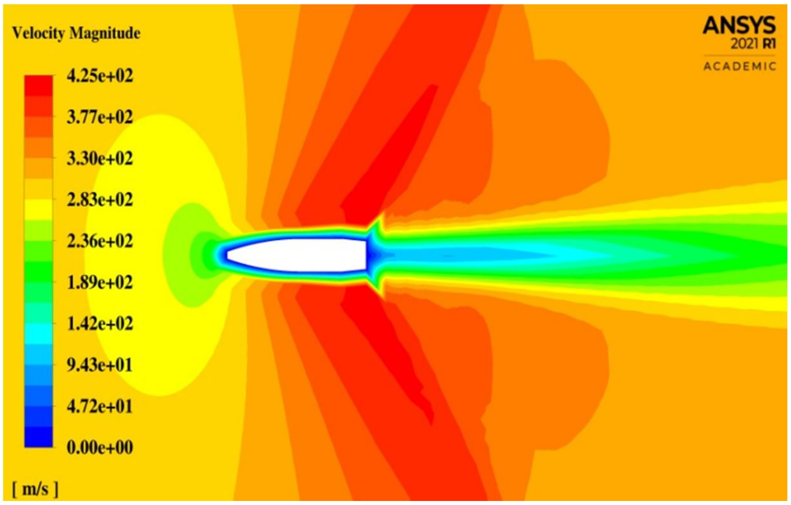

Fig 7: VELOCITY CONTOUR AT M=1

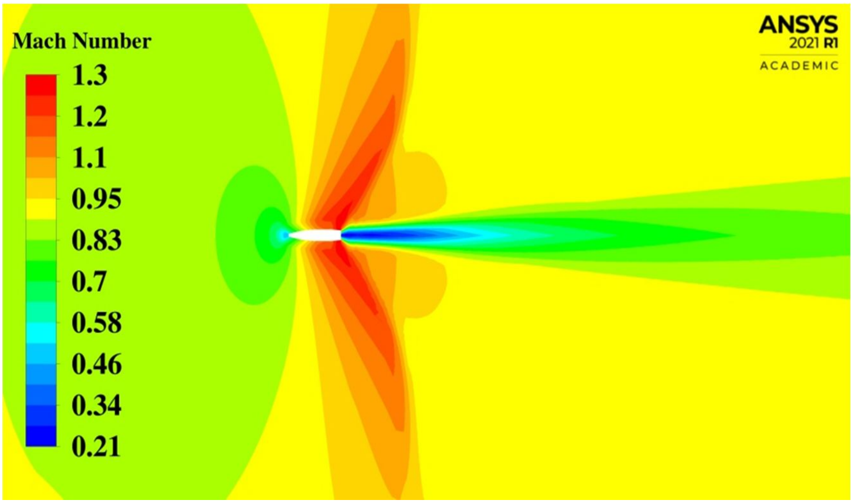

Fig 7b: Velocity Contour of Mach number profile AT M=1

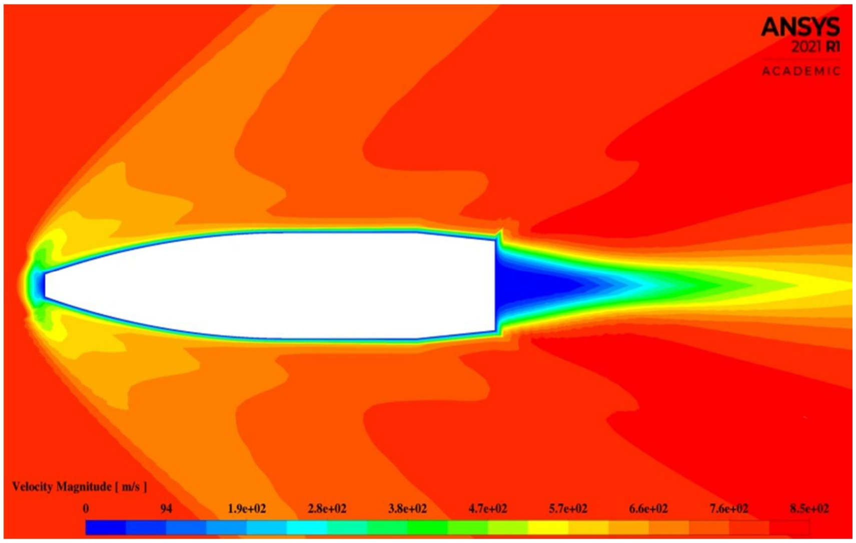

Fig 8: Velocity Contour AT M= 2.5

International Journal for Research in Applied Science & Engineering Technology (IJRASET)
ISSN: 2321-9653; IC Value: 45.98; SJ Impact Factor: 7.429
Volume 9 Issue VIII Aug 2021- Available at www.ijraset.com

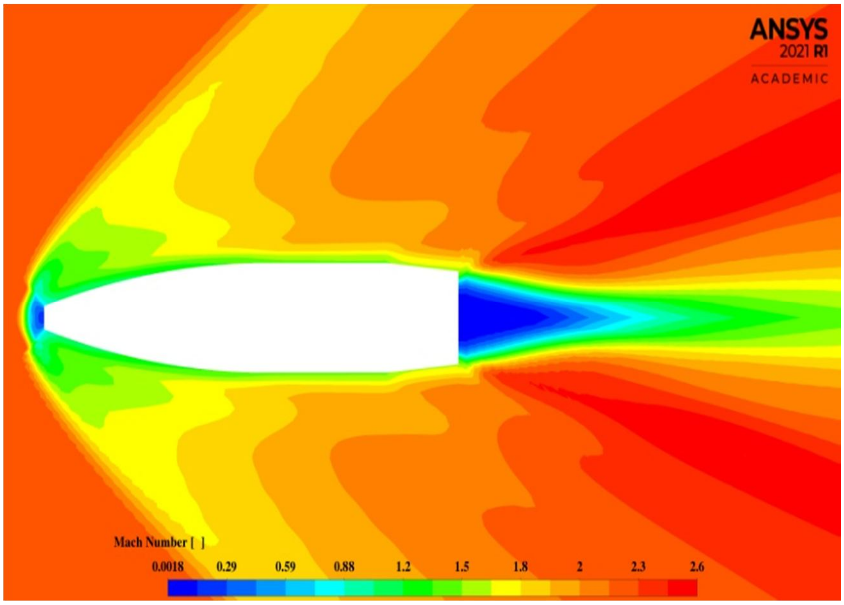

Fig 8.A: VELOCITY CONTOUR (Mach number profile) at M=2.5

In subsonic flow, Fig 9 the pressure is high over the top and bottom of the bullet. In transonic flow, FIG 10 there is a formulation of a wave over bullet; this shows bullet is going to enter supersonic from transonic. Where else in supersonic flow FIG 11 the formatting of Shock cone is generated in supersonic flow. Structured heating is less in the case of semi-tangential bullet because the attached shockwave does not affect the boundary layer & in Fig 11 we can see the bow shock transfers most of the heat generated outside of the boundary layer without interfering with the flow of the bullet

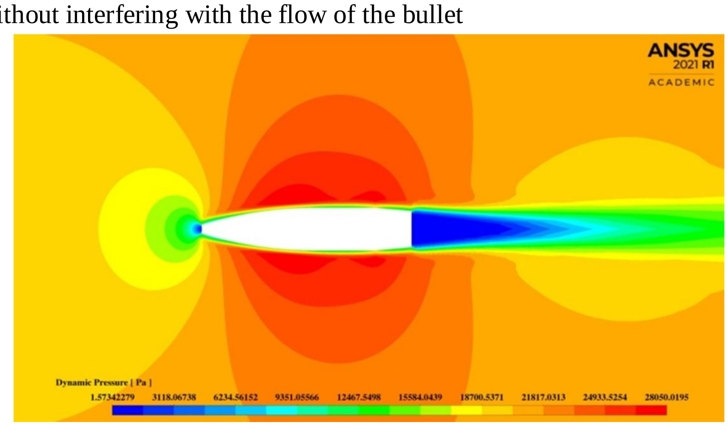

Fig 9: PRESSURE CONTOUR AT M=0.50

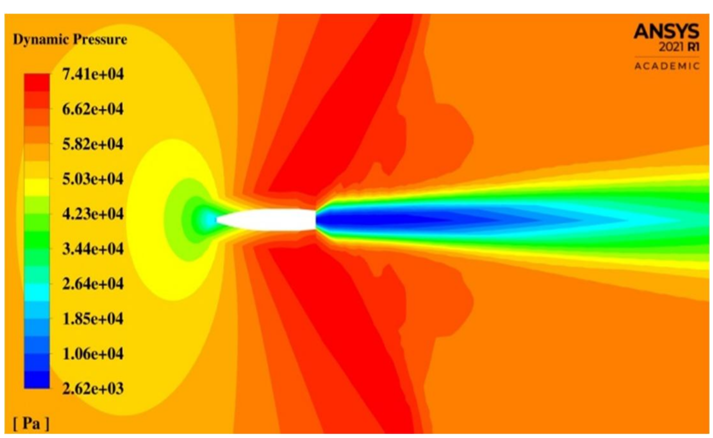

Fig 10: PRESSURE CONTOUR AT M=1

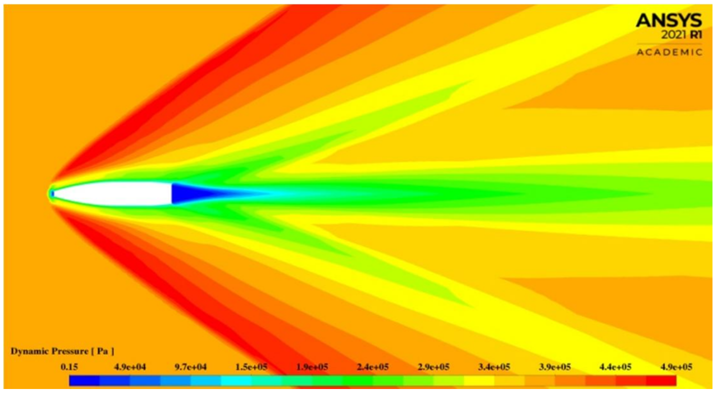

Fig 11: PRESSURE CONTOUR AT M=2.5

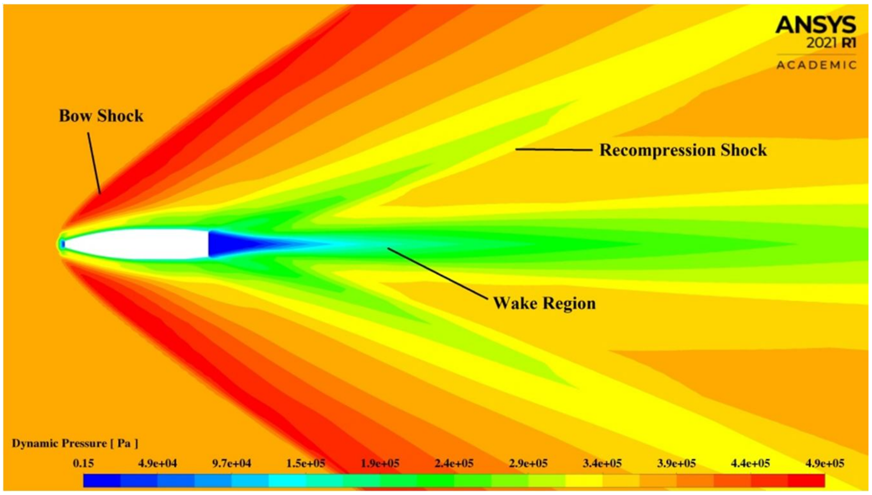

Fig 11.A : PRESSURE CONTOUR WITH SHOCKWAVE ATTACHMENT M= 2.5

In fluid dynamics, the drag is a dimensionless quantity that is used to quantify the drag or resistance of an object in a fluid environment Cd of present design is 0.345(APPEDIX 1)

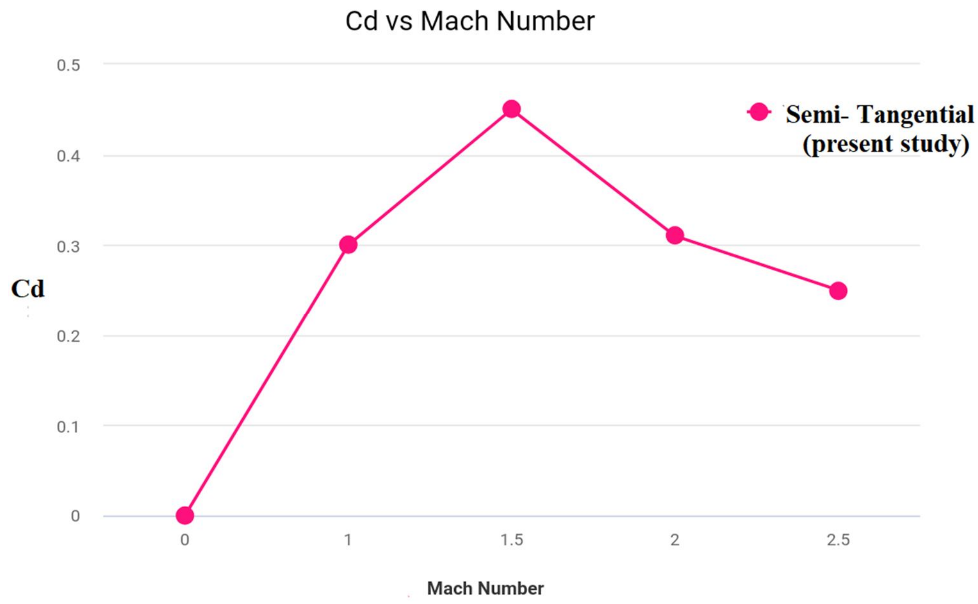

Fig 12: Cd vs Mach number

International Journal for Research in Applied Science & Engineering Technology (IJRASET)
ISSN: 2321-9653; IC Value: 45.98; SJ Impact Factor: 7.429
Volume 9 Issue VIII Aug 2021- Available at www.ijraset.com

The bullet's output is heavily influenced by the turbulence generated behind it. The length of turbulence's effect behind the projectile is determined by its viscosity ratio. Figures 13, 14, and 15 show the viscosity ratio at different Mach numbers. Turbulent flow creates more friction drag than laminar flow due to its greater interaction with the surface of the bullet body. Rough surfaces accelerate the transition of boundary layer airflow from laminar to turbulent which, in turn, increases the thickness of and the airflow disruption within the boundary layer. These increases result in more air molecules being affected by the movement of the bullet and a corresponding increase in friction drag. Friction drag can be reduced by delaying the point at which laminar flow becomes turbulent. According to Litz [1]This can be accomplished by smoothing the exposed surfaces of the bullet by using boat-tail design on the trailing edges of the bullet[4] as we can see the turbulence intensity is reduced in our semi tangential bullet from Fig 14 to 16

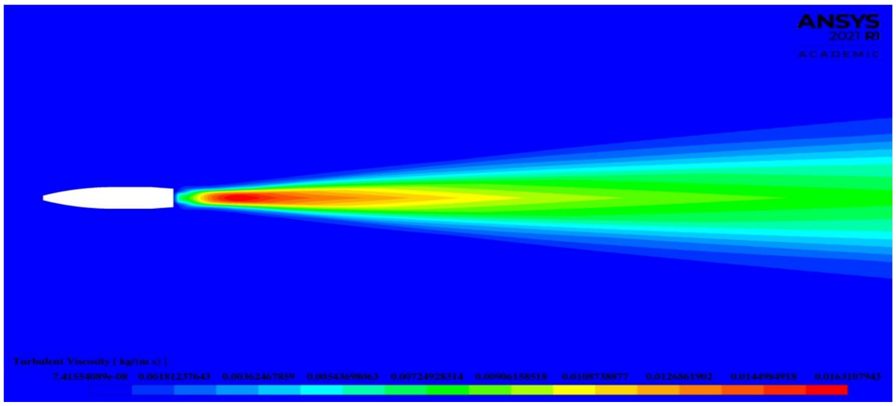

Fig 13: TURBULENCE VISCOSITY AT M=0.50

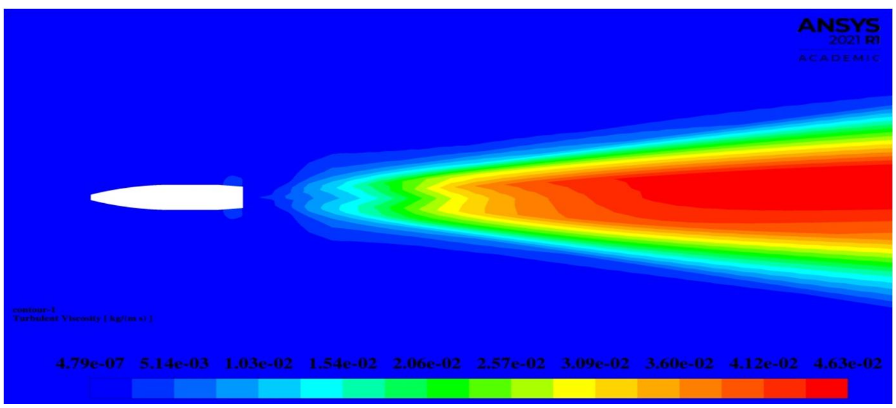

Fig 14: TURBULENCE VISCOSITY AT M=1

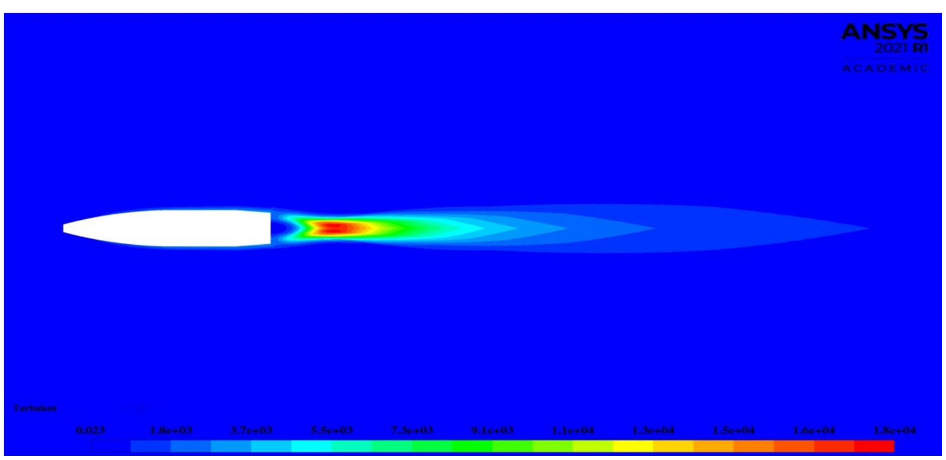

Fig 15: TURBULENCE VISCOSITY AT M=2.5

International Journal for Research in Applied Science & Engineering Technology (IJRASET)
ISSN: 2321-9653; IC Value: 45.98; SJ Impact Factor: 7.429
Volume 9 Issue VIII Aug 2021- Available at www.ijraset.com

VI. PRESENT STUDIES

In This present research study various aerodynamic parameters are been studied and carried out using CFD. The other physical performance charactertics like Cd, SG, and Time of flight of present design has been found out using Berger bullet ballistic calculator [4] and the graphs are plotted. The present study explains about the comparison of existing design with the present design Existing bullet dimension are taken from Berger bullet catalog [4] are compared with present design By doing this research various physical factor Table 4 is a comparison study of existing design with the present design, where various physical factors like bullet diameter, nose length are compared. Fig 16: discuss about the Cd values of existing design with present design.

The Physical factor like Cd, SG, and Time of flight of present design has been found out and the graphs are mentioned in Fig 1 to Fig 18

Table 4: Comparison Of Exiting Bullet Dimmesions With Present Design

TYPE	Elite Hunter 30 Caliber [4]	Hybrid Tactical Hunter 30 Caliber [4]	Semi-Tangential (Present Study)
Bullet Diameter	0.308	0.308	0.308
Boat Tail	0.272	0.227	0.217
Bearing Surface	0.542	0.633	0.490
Base to Ogive	0.883	0.942	0.788
Nose Length	0.794	0.894	0.847
Meplat	0.035	0.020	0.07

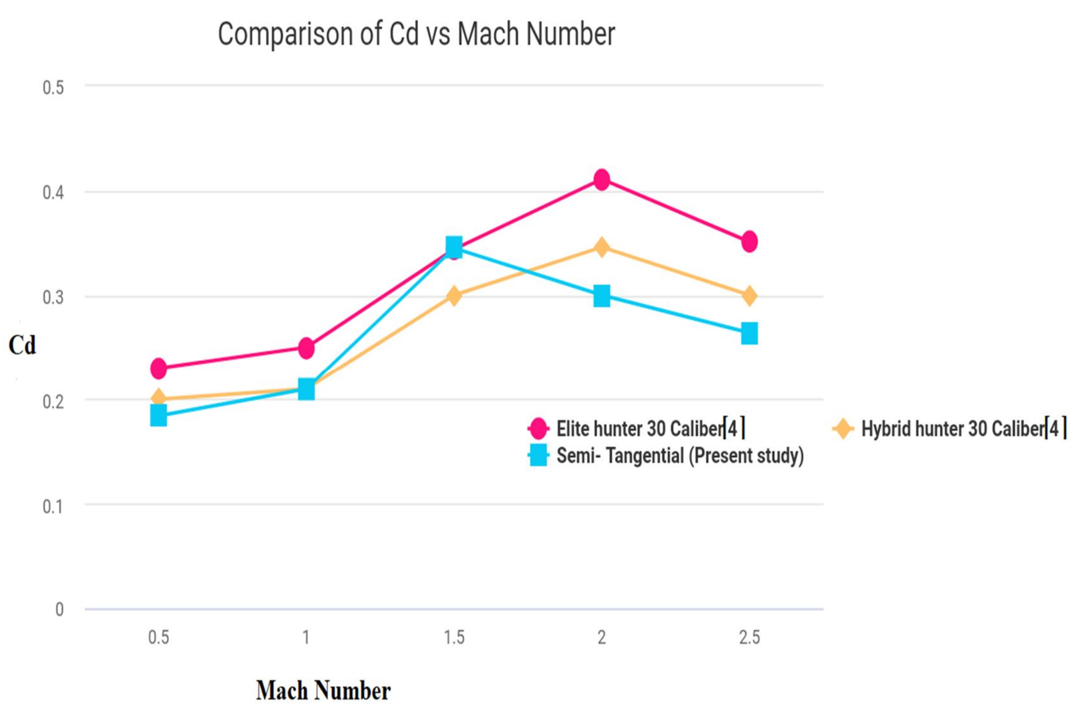

Fig 16: COMPARISON OF Cd vs Mach number

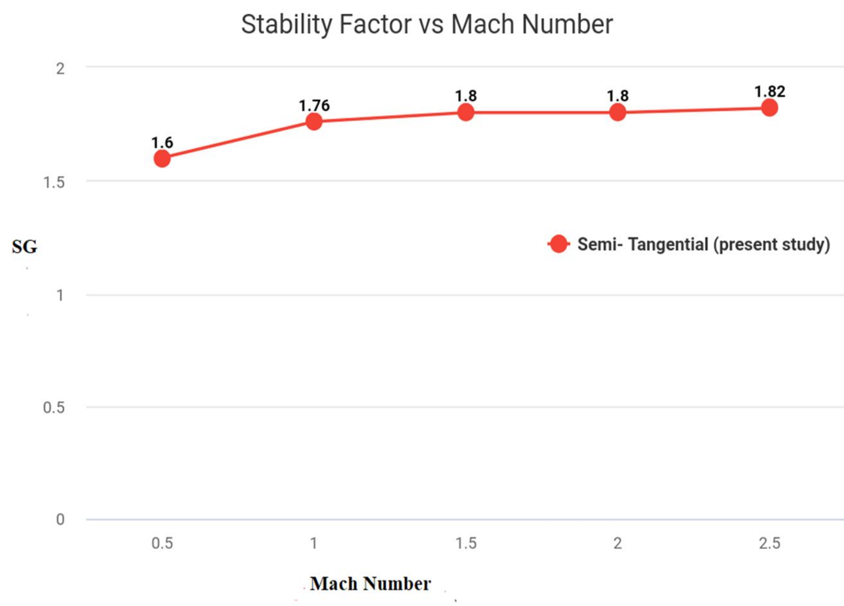

Fig 17: SG Vs Mach number

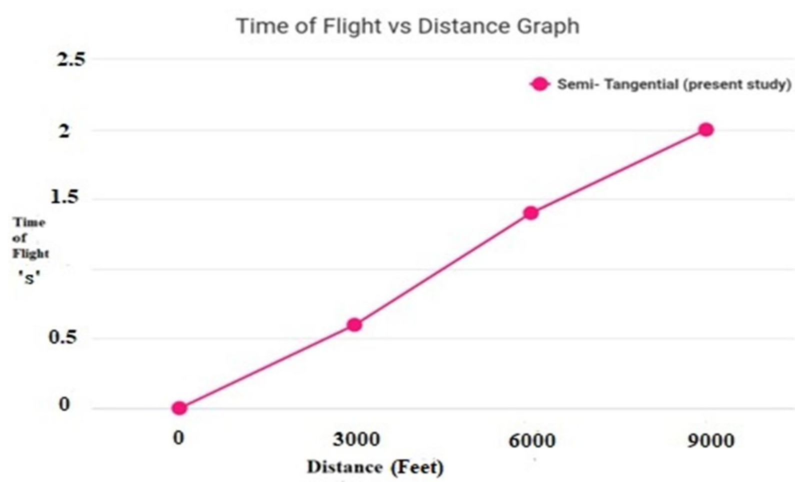

Fig 18: Time of Flight vs Distance travelled by Present study Semi Tangential bullet

VII. CONCLUSIONS

To further understand the flow/shock characteristics, a thorough quantitative analysis of the flow past a semi-tangential ogive projectile at various parameters is carried out. Other features such as shock detachment, drag coefficient, stability factor, ballistic coefficient, time of travel, and turbulence are also studied

1) In terms of shock detachment, Structural heating can be reduced if more of the heat can be shifted outside the boundary layer. Since the attached shockwave is away from the boundary layer, where else in the case of the parabolic nose, the attached shockwave is close to the boundary layer in Fig 4, which intern increases the heat of the structure. Where else in semi-tangential bullet shape the generated attached shockwave does not interfere with the boundary layer as it has been deflected away from the boundary layer, so structural heating is reduced. Formation of shockwave is along direction of bullet flow, so flow of bullet is not affected.
2) The coefficient of drag of present design is around 0.345 where existing ogive bullet drag is in the range of 0.35 to 0.4, Due to design augmentation C_d is reduced significantly
3) The turbulence generated is reduced by smoothing the exposed surface and adding a boat tail design [21] to the trailing edge.

REFERENCES

[1] Litz, Bryan Characteristics of Different Bullet Ogive Designs. [online] Appliedballisticsllc.com. Available at: <https://appliedballisticsllc.com/wp-content/uploads/2019/11/ABDOC2.1-OGIVECOMPARISON.pdf>

[2] A. Narayan, S. Narayanan and R. Kumar, "Hypersonic flow past nose cones of different geometries: a comparative study", SIMULATION, vol. 94, no. 8, pp. 665-680, 2017. Available: 10.1177

[3] D. Wilcox, "Formulation of the k-w Turbulence Model Revisited", AIAA Journal, vol. 46, no. 11, pp. 2823-2838, 2008. Available: 10.2514/1.36541

[4] Berger. Bullet Product Catalog & Berger ballistic calculator , Mesa, AZ (2020)

[5] P. R. Spalart, S. R. Allmaras. A One Equation Turbulence Model for Aerodynamic Flows. AIAA- 92-0439 (1992)

[6] R. Pircher, D. Preiß, S. Pollak, A. Thierauf-Emberger, M. Perdekamp and D. Geisenberger, "The influence of the bullet shape on the width of abrasion collars and the size of gunshot entrance holes", International Journal of Legal Medicine, vol. 131, no. 2, pp. 441-445, 2016. Available: 10.1007/s00414-016-1501-6

[7] Petzal, D., 2021. How fast is the Speeding Bullet. Field and Stream 97. [online] Iopscience.iop.org. Available at: <https://iopscience.iop.org/article/10.1088/1361-6552/ab2d33>

[8] V. Muruganantham and T. Babin, "Numerical investigation of hybrid blend design target bullets", MATEC Web of Conferences, vol. 172, p. 01006, 2018. Available: 10.1051/matecconf/201817201006

[9] V. Menezes, S. Kumar, K. Maruta, K. Reddy and K. Takayama, "Hypersonic flow over a multi-step afterbody", Shock Waves, vol. 14, no. 5-6, pp. 421-424, 2005. Available: 10.1007/s00193-005-0281-6

[10] Owens, RV. Aerodynamic characteristics of spherically blunted cones at mach numbers from 0.5 to 5.0. Washington, DC: National Aeronautics and Space Administration, 1965.

[11] Heberle, JW, Wood, GP, Gooderum, PB. Data on shape and location of detached shock waves on cones and spheres. NACA TN 2000. Washington, DC: National Aeronautics and Space Administration, January1950.

[12] J. FAY and F. RIDDELL, "Theory of Stagnation Point Heat Transfer in Dissociated Air", Journal of the Aerospace Sciences, vol. 25, no. 2, pp. 73-85, 1958. Available: 10.2514/8.7517

[13] J. Murugan and R. Govardhan, "Shock wave–boundary layer interaction in supersonic flow over a forward-facing step", Journal of Fluid Mechanics, vol. 807, pp. 258-302, 2016. Available: 10.1017/jfm.2016.574

[14] P. Seshadri and A. De, "FLOW PAST STATIONARY AND OSCILLATING AIRFOIL AT A LOW REYNOLDS NUMBER USING SHARP INTERFACE IMMERSED-BOUNDARY APPROACH", Journal of Flow Visualization and Image Processing, vol. 27, no. 1, pp. 47-69, 2020. Available: 10.1615/jflowvisimageproc.2020030995

[15] S. Torii, "PREFACE: FLOW VISUALIZATION, IMAGE PROCESSING AND RELATED TECHNIQUES", Journal of Flow Visualization and Image Processing, vol. 25, no. 1, p. v, 2018. Available: 10.1615/jflowvisimageproc.v25.i1.10.

[16] S. De, "Efficient Computation of Fluid Drag Forces on Micro machined Devices Using a Boundary Integral Equation-Based Approach", International Journal for Multiscale Computational Engineering, vol. 1, no. 2-3, p. 12, 2003. Available: 10.1615/intjmultcompeng.v1.i23.100

[17] D. Braun, H. S. Wright, and M. A. Croom, “Design of the ARES mars airplane and mission architecture,” Journal of Spacecraft and Rockets, vol. 43, no. 5, pp. 1026-1034, 2006

[18] K. Spiros, “Multi-objective optimization in spatial planning: Improving the effectiveness of multi-objective evolutionary algorithms (non-dominated sorting genetic algorithm II),” Engineering Optimization, vol. 47, no. 5, pp. 601-621, 2015

[19] Donea, J., and Huerta, A., 2004, “Finite Element Methods for Flow Problems”, John Wiley & Sons Ltd., USA, Chap. 1 and 4. Garibaldi, J., Storti, M., Battaglia, L., and D’elìa, J., 2008,

[20] Mario A. Storti “Numerical Simulations of the Flow Around a Spinning Projectile in Subsonic Regime,” Latin American Applied Research, 38, pp. 241–247.

[21] S. K, B. K, P. Selvarajan, D. P and P. V, "Drag reduction study of a 2D metal projectile series using SU2 code", 2018 Applied Aerodynamics Conference, 2018. Available: 10.2514/6.2018-4128

A. *Grain Structure*

Grain structure of a solid is an arrangement of differently oriented grains, surrounded by grain boundaries

GRAIN STRUCTURE= VOLUME OF PROJECTILE x SPECIFIC GRAVITY OF METAL USED (COPPER)

GS=266

B. *Ballistic Co-Efficent*

Ballistic Coefficient (BC) is a measure of external ballistic performance for bullets. The higher a bullets BC is, the less drop, and wind deflection it will have at all ranges for a given muzzle velocity and environment**.**

BC=0.422 (APPEX 1)

C. *Twist Rate*

Twist rate refers to the rate of spin in the rifle barrel, and is represented in inches per turn.

TR= 10.12 OR 1/10 (APPEX 1)

D. *Rpm Of Bullet*

A revolution per minute is the number of turns of bullet in one minute. It is a unit of rotational speed or the frequency of rotation around a fixed axis.

RPM = 201600 (APPEX 1)

E. *Stablity Factor*

Stability is quantified by the gyroscopic stability factor, SG.

SG=1.83 (APPEX 1)

F. *Drag Co-Efficent*

In fluid dynamics, the drag is a dimensionless quantity that is used to quantify the drag or resistance of an object in a fluid environment

Cd=0.345(APPEX 1)

APPENDIX 1

S NO	NAME OF PROJECTILE CALCULATION	FORMULA	VALUES	SOLUTATION
1	BALLISTIC CO EFFICENT	$BC = \frac{M}{Cd.A}$	M= 9 G Cd= 0.345 A=5.8 SQIN	BC= 0.422
2	GRAIN STRUCTURE	GRAIN STRUCTURE= VOLUME OF PROJECTILE x SPECIFIC GRAVITY OF METAL USED (COPPER)	V= 31IN^3 SG= 8.89	266GR
3	TWIST RATE	Twist Rate $= \frac{CD^2}{L}$ x sqrt $(\frac{SG}{10.9})$	C=150 L=1.575 SG=8.89 D= 0.308	TR= 1/10
4	RPM OF BULLET	$RPM = \frac{\text{Velocity x 720}}{\text{Twist Rate}}$	V- 2600fps TR= 10	RPM=201600
5	STABLITY FACTOR	$s = \frac{30m}{t^2 d^3\, l(1+l^2)}$	M=9G T=TR=10 D= 0.308 L= 1.575	SG=1.83
6	CO-EFFICENT OF DRAG	$\frac{m}{(BC)d^2} Cg 0.0014223 = Cd$	M=9g BC=0.422 Cg=1	Cd=0.345

APPENDIX 2

REFERENCE SHEET FOR PRESENT BULLET DESIGN

SNO	Description	Bullet diameter	Boat tail	Bearing surface	Base to ogive	Nose length	meplat	BC	OGIVE RADIUS	Twist rate
1	30 caliber 266gr semi-tangential	0.308 in	0.217 in	0.467 in	0.684 in	0.891 in	0.07in	0.422	13 X D(bullet diameter)	1:10’

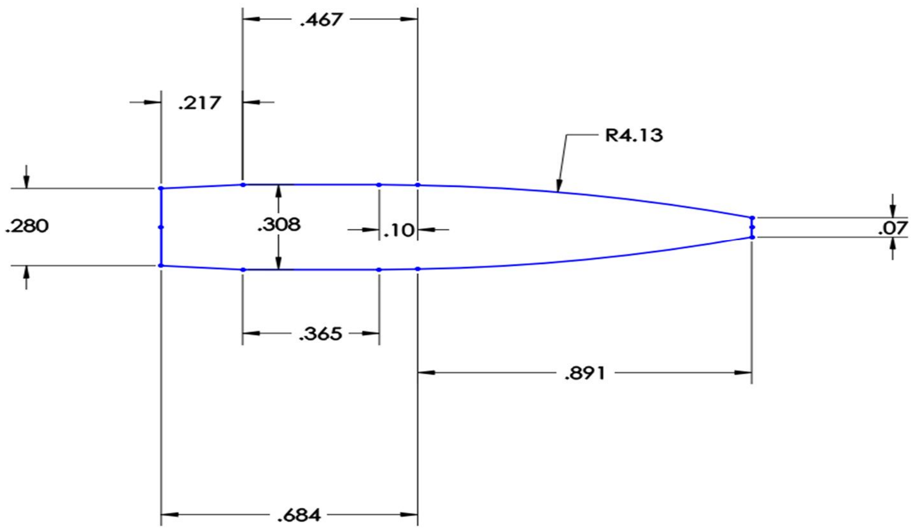

APPENDIX 3

Calculataion For Ogive Design

SNO	OGIVE TERMS	FORMULA USED	VALUES	SOLUTATION
1	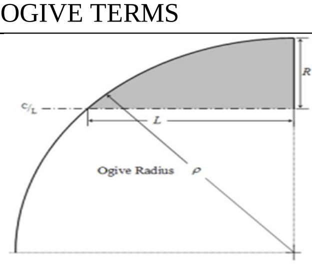	$\rho=\frac{R^2+L^2}{2R}$	R=0.308 L=1.575	ρ= 4.13
2	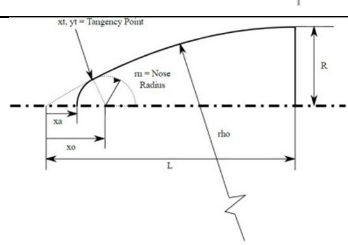	$x_a = x_0 - r_n$	X_0 =0.105 r_n =0.035	X_a=0.07